Histol Histopathol (2016) 31: 969-980

http://www.hh.um.es

Histology and Histopathology

From Cell Biology to Tissue Engineering

Transfer of mesenchymal stem cells and cyclosporine A on alkali-injured rabbit cornea using nanofiber scaffolds strongly reduces corneal neovascularization and scar formation

Cestmir Cejka[1], Jitka Cejkova[1], Peter Trosan[1,2], Alena Zajicova[1], Eva Sykova[1,3] and Vladimir Holan[1,2]

[1]Institute of Experimental Medicine, Academy of Sciences of the Czech Republic, [2]Faculty of Natural Science, Charles University and [3]Department of Neuroscience, 2nd Medical Faculty, Charles University, Prague, Czech Republic

Summary. The aim of this study was to examine whether nanofiber scaffolds seeded with rabbit bone marrow mesenchymal stem cells (MSCs nanofibers) transferred onto the damaged corneal surface and covered with cyclosporine A (CsA)-loaded nanofiber scaffolds (CsA nanofibers) enable healing of the rabbit cornea injured with 1N NaOH. The healing of damaged corneas was examined morphologically, immunohistochemically and biochemically on day 24 after the injury. Compared to untreated injured corneas, where corneal ulceration or large corneal thinning or even perforation were developed, injured corneas treated with drug free nanofibers healed without profound disturbances in a majority of cases, although with fibrosis and scar formation. In injured corneas treated with CsA nanofibers or MSCs nanofibers, the development of scar formation was reduced. Best healing results were obtained with a combination of MSCs and CsA nanofibers (MSCs-CsA nanofibers). Corneas healed with highly restored transparency. Neovascularization highly expressed in untreated injured corneas and reduced in corneas treated with CsA nanofibers or MSCs nanofibers, was suppressed in corneas treated with MSCs-CsA nanofibers. The levels of matrix metalloproteinase 9, inducible nitric oxide synthase, interleukin 6, α-smooth muscle actin, tumor growth factor β and vascular endothelial growth factor were significantly decreased in these corneas as compared to untreated corneas, where the levels of the above mentioned markers were high. In conclusion, MSCs-CsA nanofibers were effective in the treatment of severe alkali-induced corneal injury.

Key words: Alkali, Cornea, CsA nanofibers, MSCs nanofibers, MSCs-CsA nanofibers

Offprint requests to: Associate Prof. Jitka Čejková,MD,PhD,DSc, Head, Department of Eye Histochemistry and Pharmacology, Institute of Experimental Medicine, Academy of Sciences of the Czech Republic, Vídenska 1083, 14220, Prague 4,CR. e-mail: cejkova@biomed.cas.cz

DOI: 10.14670/HH-11-724

Introduction

Chemical injury of corneas, such as alkali burns, often leads to the loss of vision from corneal ulceration or perforation, or to the reduced vision from corneal healing with untransparent scar formation. Stromal fibrosis develops during the chronic phase of healing due to the increased induction of pro-inflammatory cytokines, leading to the increased expression of transforming growth factor β (TGF-β). In these processes, particularly interleukin-6 (IL-6) is involved (Luckett-Chastain and Galluci, 2009). TGF-β (existing in at least three isoforms called TGF-β1, TGF-β2, TGF-β3) is a key cytokine involved in the pathogenesis of fibrosis in many organs, whereas IL-6 plays an important role in regulation of inflammation (Zhang et al., 2005). TGF-β is necessary for the migration of cells of individual corneal layers into the damaged area and also for transdifferentiation of keratocytes into myofibroblasts, processes necessary for corneal healing (Jester et al., 2012; Dreier et al., 2013). However, when

TGF-β is overexpressed, it causes accumulation of myofibroblasts (which are less transparent than keratocytes, Jester et al., 1999) in the damaged area, resulting in corneal haze and development of untransparent scar formation. Therefore, the attempts to heal severe corneal alkali injury with at least partially restored corneal transparency have been focused on suppression of the intracorneal inflammatory response. An array of anti-inflammatory drugs has been experimentally employed for the treatment of alkali injured corneas, including corticosteroids or cyclosporine A (CsA) (Sekundo et al., 2002; Den et al., 2004; Hoffart et al., 2010; Yi et al., 2011). Holan et al. (2011) showed in the skin allograft model that CsA released from CsA nanofibers was effective in the healing of skin wounds. Recently, mesenchymal stem cells (MSCs) were used for the treatment of corneal alkali burns with promising results. MSCs promote corneal healing by secreting anti-inflammatory and growth factors (Li and Zhao, 2014). MSCs were capable of decreasing corneal inflammation by suppressing infiltration of the corneal stroma with inflammatory cells (Yao et al., 2012) and to reducing pro-inflammatory cytokines produced by macrophages (Aggarwal and Pittenger, 2005). For corneal healing, various modes of administration were employed in experimental animals. MSCs were applied systematically, topically, subconjunctivally or on amniotic membrane (Ma et al., 2006; Ye et al., 2006, 2008; Jiang et al., 2010; Yao et al., 2012). We found previously that nanofiber scaffolds were suitable carriers for MSCs. When MSCs were incubated on nanofiber scaffolds and transferred on corneas injured with alkali (0.25N NaOH), they effectively healed corneas and suppressed corneal inflammation and neovascularization (Cejkova et al., 2013). Damage of the corneal surface is more profound with more concentrated alkali. In the present study we employed highly concentrated alkali (1N NaOH) and demonstrated for the first time that nanofiber scaffolds seeded with MSCs (MSCs nanofibers) combined with CsA-loaded nanofiber scaffolds (CsA nanofibers) transferred onto the corneal surface damaged by severe alkali suppress corneal inflammation, decrease corneal neovascularization and strongly reduce corneal scar formation. This results in the corneal healing with highly restored corneal transparency.

Material and methods

Nanofiber scaffold preparation

The PLA polymer was purchased from Nature Works LLC (Minnetonka, Minneapolis, Minnesota, USA). This material was dissolved in chloroform at 7 weight percent (wt%), and two other solvents, 1,2-dichlorethane (29 wt%) and ethyl acetate (10 wt%) (both purchased from PENTA, Prague, Czech Republic), were added to this solution. The mixture was stirred until a homogenous polymer solution was obtained. For CsA nanofibers, CsA (TEVA Czech Industries, Opava, Czech Republic) was dissolved in the prepared polymer solution to selected concentrations (1, 2.5, 5 and 10 wt%) and the solution stirred until the drug was dissolved. The modified needleless Nanospider™ technology, in which polymeric jets are spontaneously formed from liquid surfaces on a rotating spinning electrode, was used for the preparation of the nanofibers. In this study, nanofiber materials with a mass per unit area of 10 g/m^2 and containing 2.5 wt% CsA were used. These nanofibers had a diameter ranging from 290-539 nm and contained 0.25 μg of CsA/mm^2. The morphology of CsA free and CsA loaded PLA nanofibers and their nanofibrous architecture were analyzed using scanning electron microscopy. We have shown previously that incorporation of CsA into the polymer solution does not influence nanofiber formation and does not have any effect on nanofiber density, diameter, porosity or architecture (Holan et al., 2011).

Mesenchymal stem cell preparation

MSCs were isolated from the bone marrow of adult New Zealand white rabbits and cultured as described for mouse MSCs (Zajicova et al., 2010). In brief, the bone marrow from the femurs and tibias was flushed out, washed and cultured in Dulbecco's modified Eagle's (DMEM) medium (PAA Laboratories, Pasching, Austria) supplemented with 10% fetal calf serum (FCS, Sigma Co., St. Louis, MO), antibiotics (100 mg/ml of streptomycin, 100 U/ml of penicillin) and 10 mM Hepes buffer. The cells were cultured at a concentration of 4x10^6 cells/ml in 6 ml of culture medium in 25 cm^2 tissue culture flasks (Nunc, Roskilde, Denmark). After a 24 h incubation period the non-adherent cells were removed by washing, and the remaining adherent cells were cultured with a regular exchange of the culture medium and passaging of the cells to maintain an optimal cell concentration. After approximately 3 weeks of culture (2-3 passages) the cells were harvested by gentle scraping and used for transplantation onto the ocular surface. For topical administration, 100 ml media containing 1x10^6 MSCs was employed.

The rabbit MSCs used in our experiments were characterized according to their adherence to plastic surfaces, by a typical fibroblast-like cell morphology, by the expression of CD73, by the absence of CD11b, and by the ability to differentiate into adipogenic and osteogenic lineages (as we have described in detail for mouse MSCs (Zajicova et al., 2010).

Nanofiber scaffolds (drug free) were cut into squares (approximately 1.5x1.5 cm) and fixed into CellCrown_24 inserts (Scaffdex, Tampere, Finland). The inserts with nanofibers were sterilized and transferred into 24 well tissue culture plates (Corning, Schiphol-Rijk, Netherlands). One hundred thousand cells in a volume of 700 ml of culture medium with 10% FCS were transferred into each well. The cells were cultured on nanofiber scaffolds for 24 h. A 10 mm diameter

nanofiber circle was cut out from the nanofiber scaffold and was used to cover corneal and limbal region.

Alkali injury of the cornea in experimental animals and nano scaffold transfer

Adult female New Zealand white rabbits (2.5-3.0 kg) were used in our experiments. The investigation was conducted according to the ARVO Statement on the Use of Animals in Ophthalmic and Vision Research. Rabbits were anesthetized by an intramuscular injection of Rometar (Xylazinum hydrochloricum, Spofa, Prague, CR, 2%, 0.2 ml/kg body weight) and Narkamon (Ketaminum hydrochloricum, Spofa, 5%, 1 ml/kg body weight).

Sodium hydroxide (1.0 N NaOH) was applied by means of a filter paper (8 mm diameter) soaked with alkali placed on the center of the cornea of right eyes for 30 s, then the eyes were immediately rinsed with tap water. The animals were divided into five groups (each group contained six rabbits). In the first group of animals, the injured eyes were left without further treatment. In the second group drug-free nanofiber scaffolds were transferred onto the injured eyes, sutured to the conjunctiva and the eyelids closed. In the third group CsA nanofibers were transferred onto the injured corneal surface, sutured to the conjunctiva and the eyelids closed. In the fourth group MSCs nanofibers were transferred with cell side facing down on the alkali injured corneal surface, sutured to conjunctiva and eyelids closed. In the fifth group MSCs nanofibers were transferred on the corneal surface, sutured to conjunctiva and covered with CsA nanofibers which were also sutured to conjunctiva and eyelids closed.

The scaffolds were sutured to conjunctiva with four interrupted sutures using 11.0 Ethilon (Ethicon, Johnson & Johnson, Livingston, England). The eyelids were closed by tarsorhapy using 1 suture of Resolon 7.0 (Resorba, Nuremberg, Germany) for 72 hours. An ophthalmic ointment compound containing bacitracin and neomycin (Ophthalmo-Framykoin, Zentiva, Prague, Czech Republic) was applied on the ocular surface for 3 days. The nanofiber scaffolds were removed from the ocular surface on day 3 after the operation. After the alkali injury and awakening from the anesthesia, the rabbits were treated with analgesia (ketoprofen, 1.0 mg/kg i.m.) two times daily for five days. The animals were sacrificed following an i.v. injection of thiopental anesthesia (Thiopental, Spofa, 30 mg/kg) after premedication with an intramuscular injection of Rometar/Narkamon. In all experiments with alkali injury, the corneas of healthy rabbit eyes served as controls. Throughout the whole experiment, photographs of the corneas were taken.

Microscopical examinations

After sacrificing the animals, the eyes were enucleated and the anterior eye segments dissected out and quenched in light petroleum chilled with an acetone-dry ice mixture. Sections were cut on a cryostat and transferred to glass slides. Subsequently, the cryostat sections were fixed in acetone at 4°C for 5 minutes. For the immunohistochemical localization of myofibroblasts, inducible nitric oxide synthase (iNOS), matrix metalloproteinase-9 (MMP9), IL-6 and vascular endothelial growth factor (VEGF), the following primary antibodies were used: monoclonal mouse anti-α SMA (Sigma, Saint Louis, MO, USA), monoclonal mouse anti-human iNOS (Biosciences, San Jose, California), goat polyclonal anti-MMP9 (Santa Cruz Biotechnology, Santa Cruz, California) monoclonal mouse anti-IL-6 (Abcam, Cambridge, UK) and monoclonal mouse anti-VEGF (Abcam). The binding of the primary antibodies was demonstrated using the HRP/DAB Ultra Vision detection system (Thermo Scientific, Fremont, California) following the instructions of the manufacturer: hydrogen peroxide block (15 minutes), ultra V block (5 minutes), primary antibody incubation (60 minutes), biotinylated goat anti-mouse IgG (Lab Vision, Fremont, California) or donkey anti-goat IgG (Santa Cruz Biotechnology) secondary antibody incubation (10 minutes) and peroxidase-labeled streptavidin incubation (10 minutes). Visualization was performed using a freshly prepared DAB substrate-chromogen solution. Cryostat sections in which the primary antibodies were omitted from the incubation media served as negative controls. Some sections were counterstained with Mayer's hematoxylin. The counting of cells positive for iNOS and IL-6 in the corneal stroma was performed by an examiner without prior knowledge of the experimental procedure. Three randomly chosen fields of corneal sections (of the same field size and the same microscope magnification) from six corneas of each experimental animal group were used. For each cornea the mean value from three fields was counted. For morphological evaluation of corneas, haematoxylin-eosin staining of post-fixed cryostat sections was employed.

Evaluation of corneal neovascularization and transparency

For evaluation of corneal neovascularization, the number of vessels was counted in each 60° sector of the corneal surface. The mean value and standard deviation were counted from five measurements. This procedure was applied for every eye from matching groups of eyes (control, injured untreated, injured and treated with drug-free nanofibers, injured and treated with MSCs nanofibers or with CsA nanofibers or with MSCs-CsA nanofibers.

Changes of corneal transparency after the injury and during healing were examined macroscopically and according to the measurement of the central corneal thickness (taken as an index of corneal hydration, Cejka et al., 2012). In brief: The central corneal thickness of anesthetized animals was measured using an ultrasonic

pachymeter SP-100 (Tomey Corporation, Nagoya, Japan) in the corneal center. The corneal thickness was measured in the same corneas before alkali injury (corneas of healthy eyes) and after the removal of nanofibers, on day 15 and 24 after the injury (all experimental groups). Each cornea was measured four times and the mean value of the thickness (in μm) and the standard deviation were computed.

Detection of gene expression by real-time PCR

The expression of genes for IL-6, TGF-β1, VEGF and iNOS in control corneas, injured untreated corneas or injured corneas treated with the drug-free nanofibers, with MSC nanofibers, CsA nanofibers or with MSCs-CsA nanofibers was determined by quantitative real-time polymerase chain reaction (PCR). Corneas were excised using Vannas scissors, transferred into Eppendorf tubes and immediately frozen. The frozen corneal tissue was then homogenized and 500 μl of TRI Reagent (Molecular Research Center, Cincinnatti, OH) was added for the RNA isolation. The details of RNA isolation, transcription and the PCR parameters have been described previously (Trosan et al., 2012). In brief, total RNA was extracted using TRI Reagent according to the manufacturer's instructions. One μg of total RNA was treated using deoxyribonuclease I (Promega) and subsequently used for reverse transcription. The first-strand cDNA was synthesized using random primers (Promega, Madison, WI) in a total reaction volume of 25 μl using M-MLV Reverse Transcriptase (Promega).

Quantitative real-time PCR was performed in an StepOnePlus real-time PCR system (Applied Biosystems). The relative quantification model with efficiency correction was applied to calculate the expression of the target gene in comparison with GAPDH used as the housekeeping gene. The following primers were used for amplification: GAPDH – 5'-CCCAACGTGTCTGTCGTG (sense), 5'- CCGACC CAGACGTACAGC (antisense), IL-6 – 5'- GGGCAA GATGATGCCAAA (sense), 5'- TTGTGATGACAGT TTGGTGAGTC (antisense), iNOS – 5'- AGGGAG TGTTGTTCCAGGTG (sense), 5'- TCCTCAACCT GCTCCTCACT (antisense), TGF-β1 – 5'- GCCTGC AAGTGCTCAAGTTAC (sense), 5'- TGCTGCATTT CTGGTACAGC (antisense), and VEGF – 5'- CGAGA CCTTGGTGGACATCT (sense), 5'- ATCTGCATGGT GACGTTGAA (antisense). The PCR parameters included denaturation at 95°C for 3 min, then 40 cycles at 95°C for 20 s, annealing at 60°C for 30 s and elongation at 72°C for 30 s. Fluorescence data were collected at each cycle after an elongation step at 80°C for 5 s and were analyzed on the StepOne Software, version 2.2.2 (Applied Biosystems). Each individual experiment was done in triplicate.

Statistics

Analysis of data showed normal distribution and the results are expressed as mean ± SD. Comparisons between two groups were made by Student t-test, and multiple comparisons were analyzed by ANOVA. A value of $p<0.05$ was considered statistically significant. For corneal thickness, paired t-test was employed.

Results

Haematoxylin eosin staining (HE), immunohistochemical expression and gene expression of MMP9, iNOS and IL-6 in alkali-injured corneas on day 24 after the injury

In the untreated injured corneas ulcers developed or corneas were largely thinned or perforated. Corneas were vascularized (Fig. 1A). In these corneas high expression of MMP9 was seen (Fig. 1B). A very similar picture was observed in injured corneas treated with nanofiber scaffolds (drug free) (Fig. 1C,D), however corneas were partially reepithelialized. In injured corneas treated with CsA nanofibers or MSCs nanofibers MMP9 expression (Fig. 1F,H) and corneal neovascularization (Fig. 1E,G) were reduced. In injured corneas treated with both nanofibers (MSCs-CsA) corneal neovascularization (Fig. 1I) and MMP9 expression (Fig. 1J) were low compared with healthy cornea (Control) (Fig. 1K,L), where MMP9 expression is nearly absent. The numbers of positive cells for MPP9 expression are shown in Fig. 1M. High numbers of positive cells present in untreated corneas decrease in corneas treated with drug-free nanofibers, CsA nanofibers, MSCs nanofibers and MSCs-CsA nanofibers. The expression of iNOS (Fig. 2A) and IL-6 (Fig. 2B) was high in injured untreated corneas (vascularized and without epithelium) and in injured corneas treated with drug free nanofibers (Fig. 2C,D). Expression of iNOS and IL-6 was reduced in injured corneas treated with CsA nanofibers (Fig. 2E,F) or MSCs nanofibers (Fig. 2G,H). In injured corneas treated with both nanofibers (MSCs-CsA) iNOS expression (Fig. 2I) and IL-6 expression (Fig. 2J) were low compared with healthy (Control) cornea (Fig. 2K,L), where iNOS and IL-6 expressions were absent. The numbers of positive cells for iNOS and IL-6 expression are shown in Fig. 2M,O. High numbers of positive cells appearing in untreated corneas progressively decrease in corneas treated with drug-free nanofibers, CsA nanofibers, MSCs nanofibers and MSCs-CsA nanofibers. The expression of genes for iNOS and IL6 are summarized in Fig. 2N,P. The treatment of injured corneas with CsA-loaded nanofibers (CsA) and particularly with MSCs nanofibers (MSCs) reduced the gene expression. Best results in gene suppression were obtained with the treatment of injured corneas with both nanofibers (MSCs-CsA).

Immunohistochemical expression and gene expression of α-SMA, VEGF and TGF-β1 in alkali-injured corneas on day 24 after the injury

The expression of α-SMA was high in untreated

injured cornea (without epithelium) (Fig. 3A) and also in injured corneas treated with nanofibers (drug free) (Fig. 3C). In both cases the fibrous retrocorneal membrane was developed (Fig. 3B,D). CsA nanofiber treatment (Fig. 3E) and particularly MSCs nanofiber treatment (Fig. 3G) decreased the expression of α-SMA in the corneal stroma and inhibited the development of retrocorneal membrane (Fig. 3F,H). In injured corneas treated with both nanofibers (MSCs- CsA), α-SMA expression was strongly suppressed (Fig. 3I) and the retrocorneal membrane was absent (Fig. 3J). In healthy corneas (Control) (Fig. 3K,L) α-SMA expression was lacking. The numbers of positive cells for α-SMA expression are shown in Fig. 3M. High numbers of positive cells appearing in untreated corneas progressively decrease in corneas treated with drug-free nanofibers, CsA nanofibers, MSCs nanofibers and MSCs-CsA nanofibers. The expression of genes for TGF-β1 on day 24 after the injury was determined by real-time PCR and expressed in (N). The decrease of TGF-β1 expression after CsA or MSCs nanofiber treatment and particularly after CsA-MSCs nanofiber tretment corresponded with the decrease of α-SMA expression (N) in similarly treated corneas. VEGF expression was high in untreated injured corneas (Fig. 4A). Compared with these corneas, VEGF expression was decreased in injured corneas treated with drug free nanofibers (Fig. 4B), and highly reduced in injured corneas treated with CsA nanofibers (Fig. 4C) or with MSCs nanofibers (Fig. 4D). Low expression of VEGF was present in injured corneas treated with a combination of nanofibers (MSCs-CsA) (Fig. 4E). In healthy corneas (Control) VEGF expression was nearly absent. The numbers of positive expressions for VEGF are shown in Fig. 4G. High numbers of positive VEGF expression appearing in untreated corneas decreased in corneas treated with drug-free nanofibers, CsA nanofibers or MSCs nanofibers and MSCs-CsA nanofibers.

Representative images of alkali-injured rabbit eyes

Immediately after the alkali injury corneal trans-

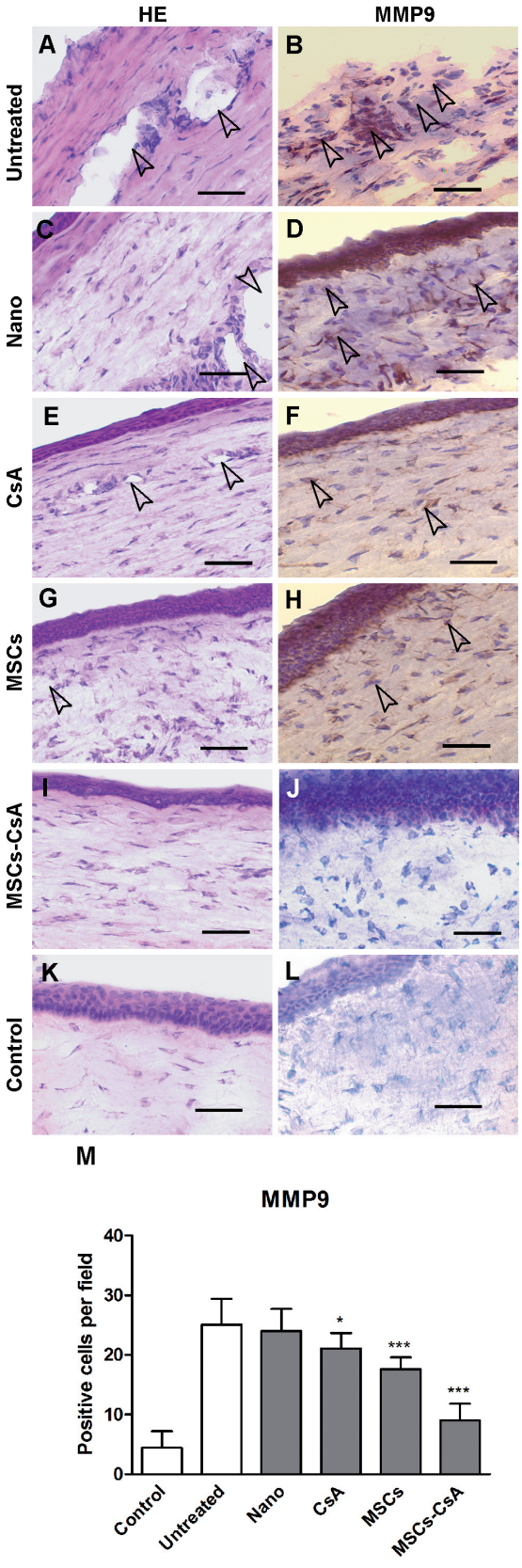

Fig. 1. Haematoxylin-eosin staining and immunohistochemical detection of MMP9 in corneas on day 24 after injury. The untreated corneas were highly thinned and vascularized (arrows) **(A).** The number of cells with MMP9 expression **(B)** was high (arrows) in these corneas. A similar microscopical picture was found in drug-free nanofiber treated corneas **(C, D)**, however the injured areas were reepithelialzed. In corneas treated with CsA nanofibers **(E, F)** or MSCs nanofibers **(G, H)**, corneal neovascularization (arrows) and MMP9 expressions (arrows) were reduced. The best results were obtained in corneas treated with MSCs-CsA nanofibers. The morphological picture **(I)** and MMP9 expression **(J)** were similar to control corneas **(K, L)**. The numbers of positive cells for MPP9 expression are shown in **M**. The values with asterisks are significantly different (*P<0.05, ***P<0.001) from injured untreated corneas. Scale bar 50 μm.

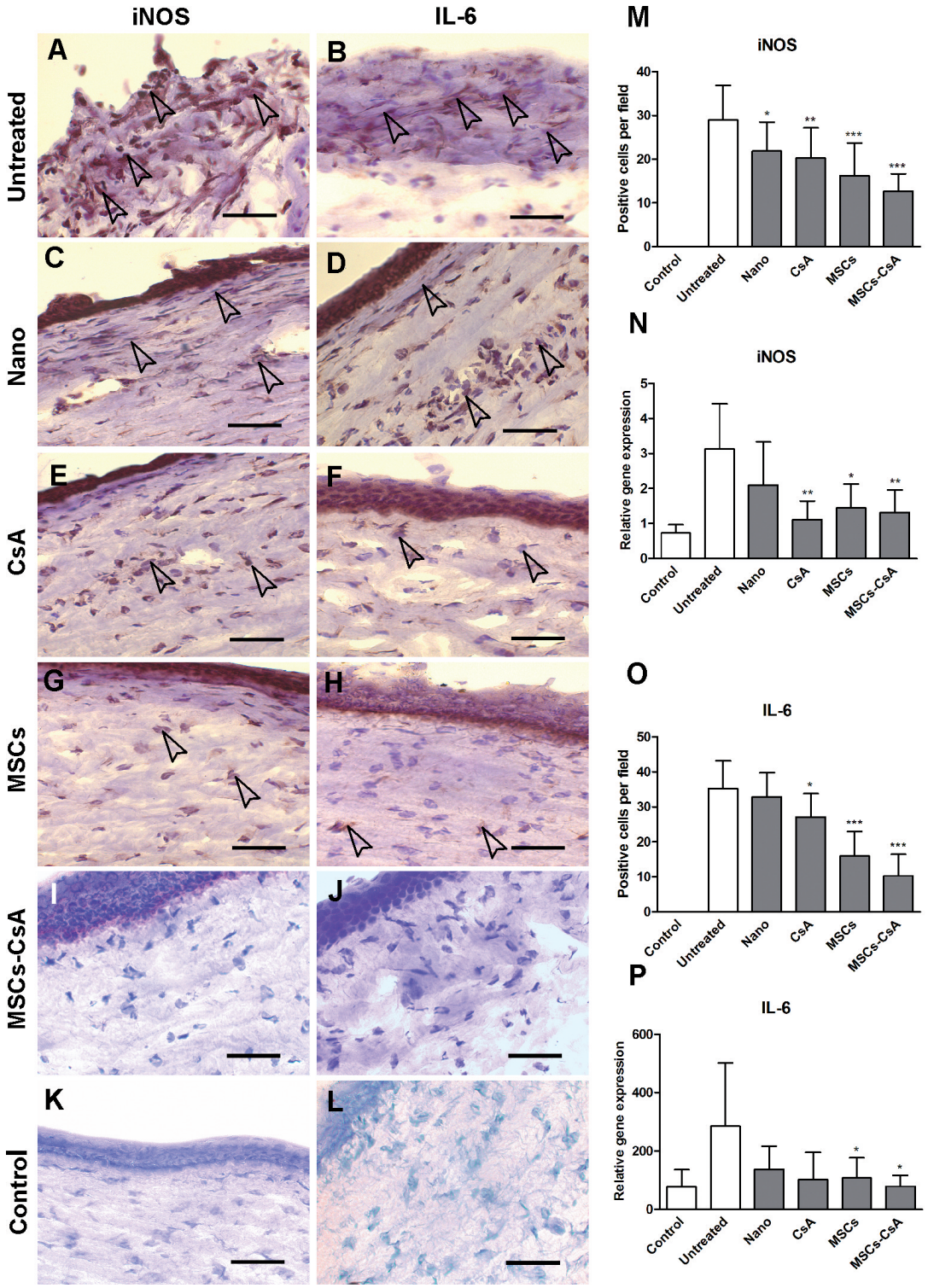

Fig. 2. Immunohistochemical detection of iNOS and IL-6 expressions in corneas on day 24 after injury. The untreated corneas were without epithelium in the injured area and corneas were vascularized. The numbers of cells with expressions of iNOS **(A)** or IL-6 **(B)** (arrows) were high in these corneas. In corneas treated with CsA nanofibers **(E, F)** or MSCs nanofibers **(G, H)** the levels of iNOS and IL-6 expression were decreased and in corneas treated with MSCs-CsA nanofibers iNOS **(I)** and IL-6 **(J)** expression was highly suppressed. Compare with control corneas **(K, L),** where iNOS or IL-6 expressions were absent and corneas stained with counterstaining only. Quantification of the number of positive cells for iNOS and IL-6 is summarized in **(M, O)**. The treatment of corneas with CsA nanofibers or MSCs nanofibers significantly decreased the numbers of positive iNOS and IL-6 cells. Best results were obtained with the treatment of corneas with MSCs-CsA nanofibers. The values with asterisks are significantly different (*P<0.05, **P<0.01, ***P<0.001) from untreated corneas. The expression of genes for iNOS **(N)** and IL-6 **(P)** on day 24 after injury was determined by real-time PCR. Each bar represents the mean ± SD from 6 individual corneas. The values with asterisks represent statistically significant difference from injured untreated corneas (*P<0.05, **P<0.01). Scale bar 50 µm.

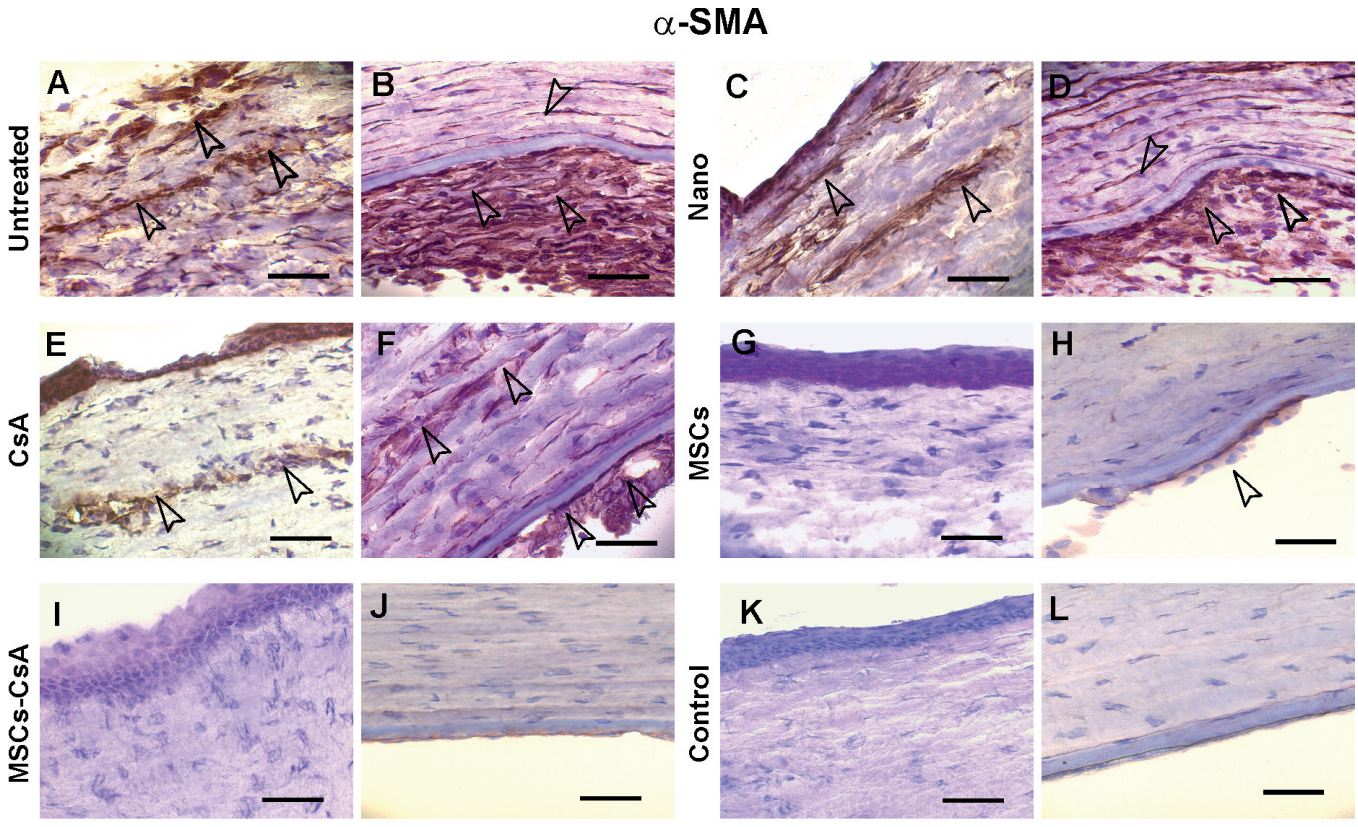

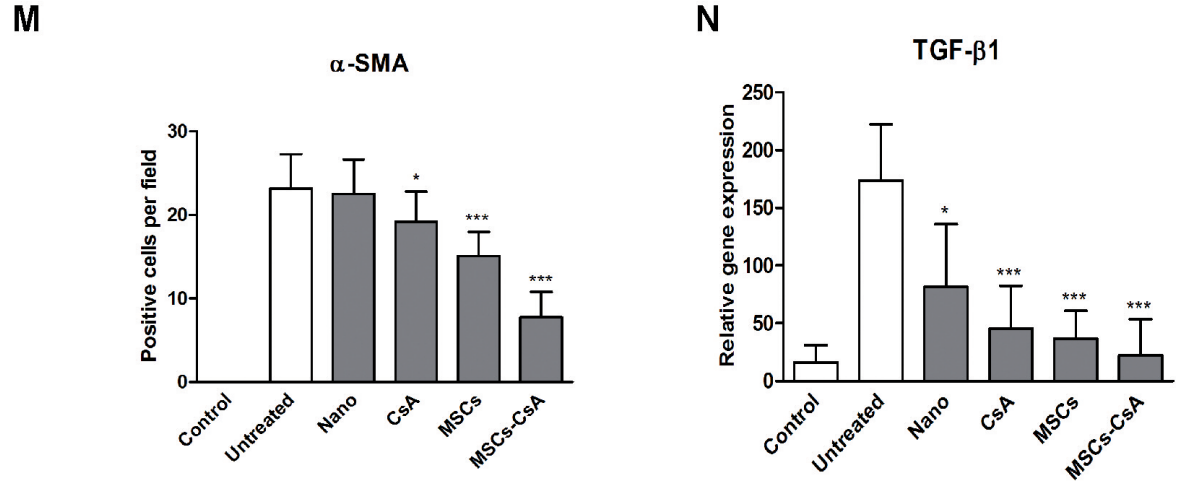

Fig. 3. Immunohistochemical detection of α-SMA expressions in corneas on day 24 after the injury. The level of α-SMA expression (a marker for myofibroblasts) was high in untreated corneas (arrows) **(A)** and in retrocorneal membrane **(B)** (arrows) in the same cornea. A very similar immunohistochemical picture was seen in corneas after the treatment with drug-free nanofibers **(C, D)**. In corneas treated with CsA nanofibers **(E, F)** and particularly with MSCs nanofibers **(G, H)** the level of α-SMA expression decreased and the development of retrocorneal membrane was suppressed (arrows). The level of α-SMA in corneas treated with MSCs-CsA nanofibers was low. Compare with control corneas **(K, L)** where α-SMA expressions were absent. Quantification of the number of positive cells for a-SMA is summarized in **(M)**. The treatment of corneas with CsA nanofibers or MSCs nanofibers significantly decreased the numbers of α-SMA positive cells. Best results were obtained with the treatment of corneas with MSCs-CsA nanofibers. The values with asterisks are significantly different (*P<0.05, ***P<0.001) from untreated corneas. The expression of genes for TGF-β1 on day 24 after injury was determined by real-time PCR and expressed in **(N)**. Each bar represents the mean ± SD from 6 individual corneas. The values with asterisks represent statistically significant difference from injured untreated corneas (*P<0.05, ***P<0.001). The decrease of TGF β1 (found biochemically) in differently treated injured corneas **(N)** corresponded with the decrease of α-SMA (detected immunohistochemically) in similarly treated injured corneas **(M)**. Scale bar 50 μm.

parency was lost. The cornea turned white in the burned area (Fig. 5B). This was in contrast to the transparent cornea of healthy eye (Fig. 5A). Fig. 5C shows MSCs-CsA nanofibers transferred onto the damaged corneal surface and sutured to the conjunctiva. The following images show the healing of corneas on day 24 after the injury: In untreated injured corneas profound perforation appeared (Fig. 5D). When the injured corneas were treated with drug free nanofibers, the corneas healed without perforations, although with profound vascularization and opacification (Fig. 5E). In injured corneas treated with CsA-nanofibers (Fig. 5F) or MSCs-nanofibers (Fig. 5G), corneal neovascularization and corneal haze were reduced. The injured corneas treated with both nanofibers (MSCs-CsA) healed with a large restoration of corneal transparency. Corneal neovascularization was strongly suppressed (Fig. 5H). Quantification of corneal neovascularization is summarized in Fig. 5I. The number of vessels high in injured untreated corneas (Untreated) and partially decreased in injured corneas treated with nano drug free (Nano), gradually decreased in injured corneas treated with CsA nanofibers (CsA), MSCs nanofibers (MSCs) and with MSCs-CsA nanofibers (MSCs-CsA).

Determination of the central corneal thickness

The levels of the central corneal thickness measured using the ultrasonic pachymeter are summarized in Fig. 6. The levels elevated after injury, decreased on day 5 and 15. On day 24 after the injury, the central corneal thickness remained significantly increased compared to levels before injury (day 0) in all cases (untreated corneas or treated corneas) with the exception of corneas treated with CsA-MSCs nanofibers, where the levels of central corneal thickness returned to levels before injury.

Discussion

Our results show that MSCs-CsA nanofiber treatment accelerated healing of seriously damaged cornea, reduced corneal inflammation, decreased corneal neovascularization and suppressed the development of untransparent scar formation.

Severe alkali burns lead to the loss of vision from the development of corneal ulceration, profound thinning or perforation of the cornea, appearing usually at the end of the 3rd week after the injury. In this study, these corneal defects developed in untreated injured corneas. In alkali-injured corneas treated with drug free nanofibers, corneas healed without ulcers or perforation, although with fibrosis and scarring. In corneas high expressions of α–SMA (a marker of myofibroblasts) were present (Fig. 3). Myofibroblasts differentiate from stromal keratocytes in the close vicinity of the wound (Jester et al., 2012). Although myofibroblasts are necessary for corneal healing (one of their main functions is wound contraction), their accumulation and persistence in injured areas is associated with corneal scarring, particularly due to their diminished crystallin protein production (and thus lower transparency) compared to keratocytes (Jester et al., 1999).

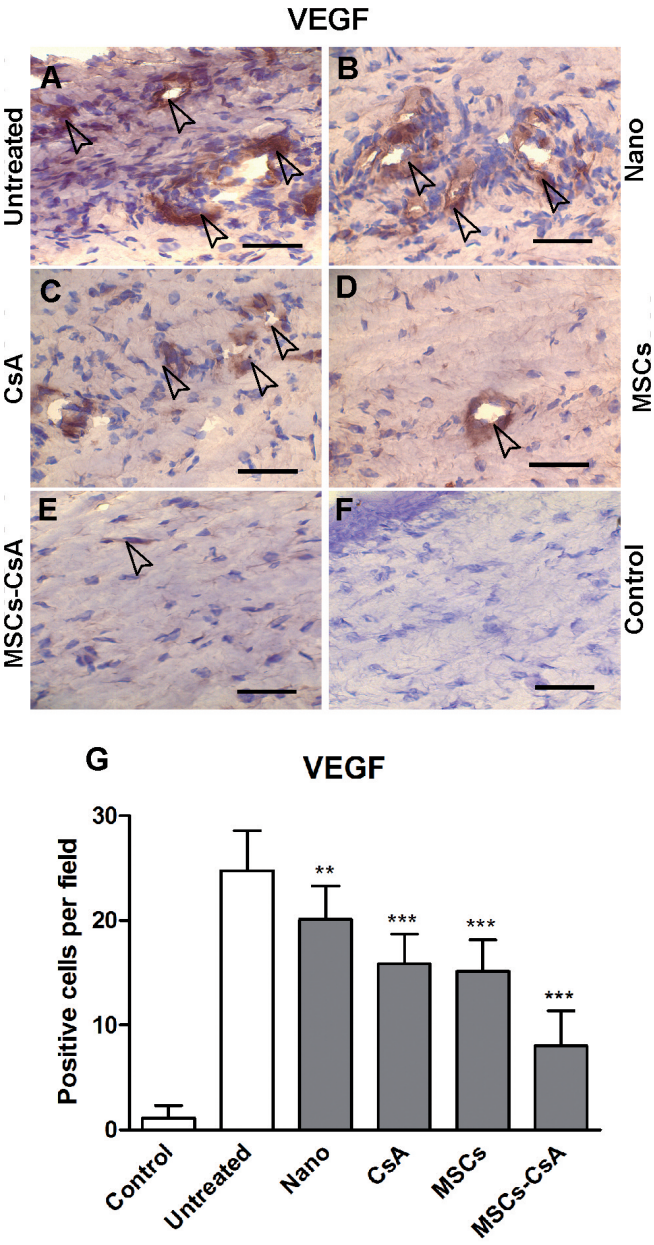

Fig. 4. Immunohistochemical detection of VEGF expressions and corneal neovascularization on day 24 after injury. VEGF expression was strong in untreated corneas **(A)** and decreased in corneas treated with nano drug free **(B)** and particulary in corneas treated with CsA nanofibers **(C)** or with MSCs nanofibers **(D).** The expression of VEGF was very low in corneas treated with MSCs-CsA nanofibers **(E)**. Compare with control corneas **(F)**. Quantification of the level of positive expression for VEGF is summarized in **(G)**. The values with asterisks are significantly different (**P<0.01, ***P<0.001) from injured untreated corneas.

Myofibroblasts produce the anomalous extracellular matrix which contributes to corneal opacity (Wilson, 2012). In our study, in alkali injured corneas treated with CsA nanofibers and particularly with MSCs nanofibers, the development of fibrosis was reduced. However, after the treatment with MSCs-CsA nanofibers, damaged corneas healed with largely restored corneal transparency (Fig. 5). In the injured part of the corneal stroma the level of α-SMA expression was reduced (Fig. 3). Myofibroblasts express high levels of α-SMA (Ishizaki et al., 1993; Dreier et al., 2013; Yang et al., 2013) and are modulated by pro-inflammatory cytokines, particularly by IL-6 (Luckett-Chastain and Galluci, 2009). In untreated injured corneas high expression of IL-6 was present (Fig. 2). Similar results were described with IL-1β (Wilson, 2012).

Myofibroblasts produce nitric oxide by iNOS in response to cytokine stimulation (Wu et al., 2013). Also corneal cells and inflammatory cells express iNOS in diseased corneas (Buddi et al., 2002). This is in accord with our findings. High expression of iNOS was present in untreated alkali-injured corneas, whereas in injured corneas treated with MSCs-CsA nanofibers, iNOS expression was highly reduced, more than after the treatment of injured corneas with CsA nanofibers or MSCs nanofibers (Fig. 2).

After severe corneal alkali injury CD3 cells and other inflammatory cells infiltrate the corneal stroma. CsA is a potent anti-inflammatory agent. It decreases inflammation and reactive oxygen species-production (Pottecher et al., 2013). In ophthalmology, CsA has usually been used in clinical practice in eye drops or ointment at concentrations between 0.05% and 2.5%. The disadvantage of this treatment is the necessity of frequent administration for the washout of drugs from the ocular surface. Holan et al. (2011) showed in the skin allograft model that CsA incorporated into nanofibers fabricated by the original needleless eletrospinning technology from a biocompatible polymer, poly(L-lactic

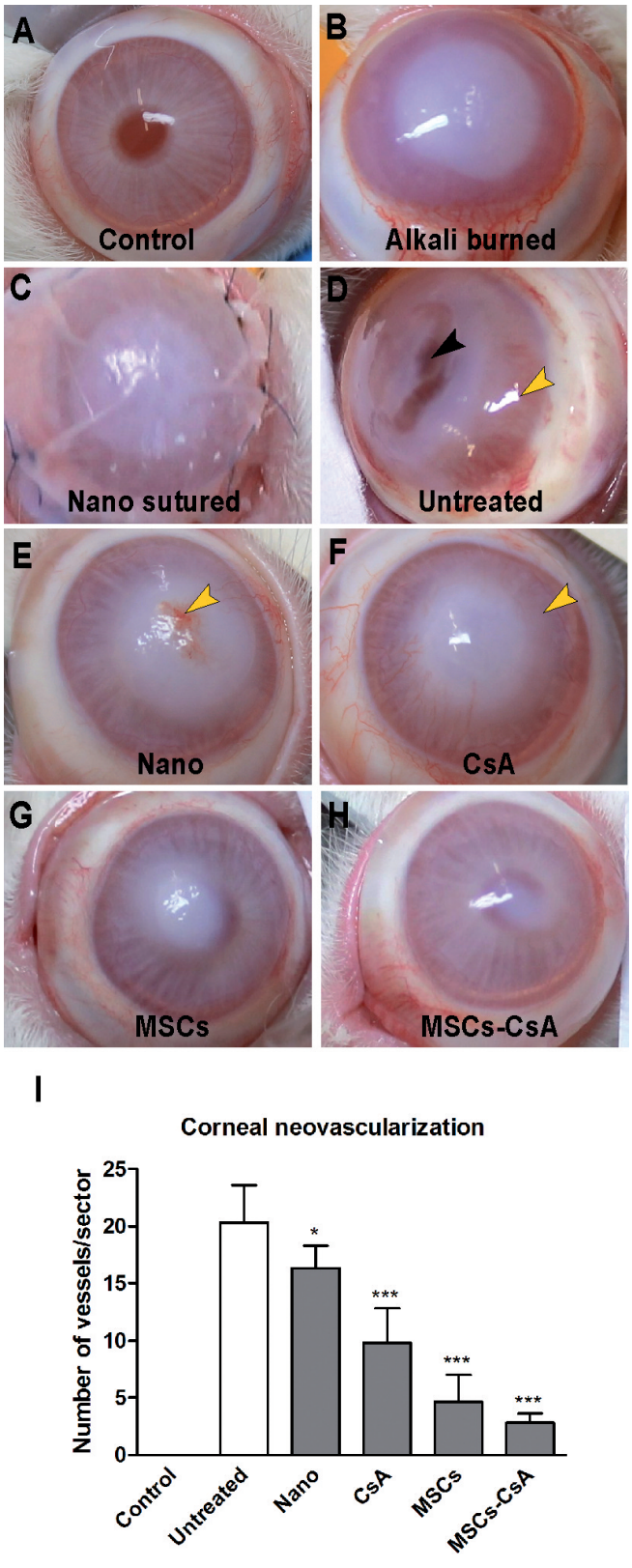

Fig. 5. Representative photographs of healthy and injured treated eyes. In comparison to healthy transparent corneas **(A)**, corneal transparency was lost in the injured area immediately after the alkali injury **(B)**. In **(C)** the injured eye was covered with MSCs-CsA nanofibers and the nanofibers were sutured to the conjunctiva. On day 24 after the injury, the untreated corneas **(D)** were thinned or even perforated (black arrow) in the burned area and corneas were highly vascularized (yellow arrow). After treatment of the injured corneas with nano drug free the vascularized corneas (arrow) were healed with large opalescency **(E).** Treatment of injured corneas with CsA nanofibers **(F)** and particularly with MSCs nanofibers **(G)** reduced both corneal haze and corneal neovascularization (yellow arrows). The injured corneas treated with MSCs-CsA nanofibers **(H)** healed with highly suppressed corneal neovascularization and with the restoration of corneal transparency. The quantification of corneal neovascularization is shown in **(I)**. Each bar represents the mean ± SD from 6 corneas. The values with asterisks are significantly different (*P<0.05, ***P<0.001) from injured untreated corneas.

acid) (PLA), was effective for the local suppression of T cell-mediated immune reactions. In this paper we describe that CsA nanofibers effectively reduce the inflammation of corneas injured with severe alkali. Moreover, we show for the first time that CsA nanofibers can be successfully combined with nanofibers on which MSCs are incubated. MSCs nanofibers transferred onto the damaged corneal surface reduced corneal inflammation and scar formation, although when combined with CsA nanofibers, the healing effect was potentiated (Figs. 1- 3).

A combination of CsA nanofibers with MSCs nanofibers significantly enabled corneal reepithelialization. After this treatment the expression of MMP9 and proinflammatory cytokines were highly decreased in the corneal epithelium (Fig. 1). Following corneal wounding, the failure of the cornea to reepithelialize is supposed to be associated with increased levels of MMP9 (Gordon et al., 2009). The reduction of MMP9 levels contributes to the remodelling of corneal basement membrane necessary for corneal reepithelialization. Also overexpression of TGF-β evoked due to the high pro-inflammatory cytokine induction after alkali injury correlates with poor reepithelialization (Haber et al., 2003; Seoane, 2006). The elevation of pro-inflammatory cytokines in poorly regenerated corneal epithelium after alkali injury was described already by Sotozono et al. (1997). To suppress high induction of pro-inflammatory cytokines is very important because pro-inflammatory cytokines are associated with the development of corneal neovascularization (Sotozono et al., 1999). In this study we show that the profound neovascularization seen in untreated alkali- injured corneas was most effectively suppressed after the treatment with MSCs-CsA nanofibers (Fig. 5).

The development of retrocorneal membrane after severe corneal alkali injury seriously threatens vision (e.g. Ishizaki et al., 1993). Highly concentrated alkali damages not only the corneal epithelium and corneal stroma, but also the endothelium. During healing of alkali-injured corneas the fibrous structure is formed in the endothelial layer beneath Descemett's membrane (Sumioka et al., 2008). According to this author during fibrogenic reaction, corneal endothelial cells undergo mesenchymal transition and transform to myofibroblasts. TGF-β is believed to be highly involved in these processes. In our studies, the retrocorneal membrane formed in untreated injured corneas was not developed in injured corneas treated with MSCs-CsA nanofibers (Fig. 3).

The disappearance of myofibroblasts from alkali-injured corneal zone is necessary for the restoration of corneal transparency. Myofibroblasts can trans-differentiate back to keratocytes or they disappear by apoptosis (Wilson, 2012). However, even when myofibroblasts disappear, the disorganized extracellular matrix produced by these cells remains and must be removed by keratocytes to restore transparency (Jester et al., 2012).

In conclusion, MSCs-CsA nanofibers proved to be effective in the treatment of alkali-injured corneas. Corneal inflammation and neovascularization were suppressed via the decrease of pro-inflammatory cytokine induction. TGF-β generation was diminished (Fig. 3) leading to reduction of untransparent scar formation. The levels of central corneal thickness elevated after the injury returned to levels before injury (Fig. 6). Corneal transparency was largely restored.

Acknowledgements. This work was supported by grant 14-12580S from the Grant Agency of the Czech Republic, grant NT/14102 from the Grant Agency of the Ministry of Health of the Czech Republic, Biocev projects CZ.1.05/1.1.00/02.0109 and CZ.2.16/3.1.00/21528 and project NPUI: LO1309.

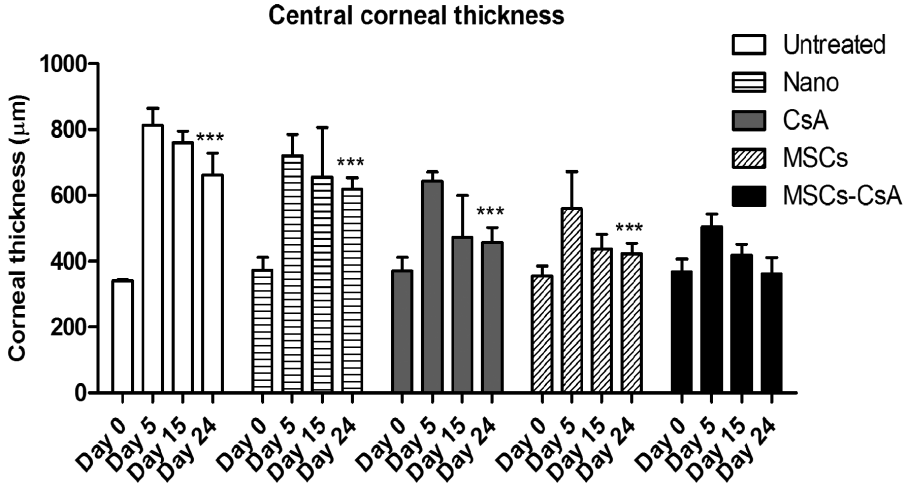

Fig. 6. Central corneal thickness of corneas. The corneas were injured with alkali and untreated, treated with nanofiber scaffold (Nano) or with nanofiber scaffolds with CsA, or MSCs, or MSCs-CsA. Central corneal thickness was measured in the same rabbit before injury (day 0) and on days 5, 15 and 24 after injury. Each bar represents the mean ± SD from 6 corneas. The values with arterisks for day 24 after the injury are statistically different (*** P<0.001) from the values before injury (day 0). On day 24 after the injury, the central corneal thickness returned to values before injury (day 0) only after the treatment of corneas with MSCs-CsA nanofibers.

References

Aggarwal S. and Pittenger M.F. (2005). Human mesenchymal stem cells modulate allogeneic immune cell responses. Blood 105, 1815-1822.

Buddi R., Lin B., Atilano S.R., Zorapapel N.C., Kenney M.C. and Brown D.J. (2002). Evidence of oxidative stress in human corneal diseases. J. Histochem. Cytochem. 50, 341-351.

Cejka C., Luyckx J. and Cejkova J. (2012). Central corneal thickness considered an index of corneal hydration of the UVB irradiated rabbit cornea as influenced by UVB absorber. Physiol. Res. 61, 299-306.

Cejkova J., Trosan P., Cejka C., Lencova A., Zajicova A., Javorkova E., Kubinova S., Sykova E. and Holan V. (2013). Suppression of alkali-induced oxidative injury in the cornea by mesenchymal stem cells growing on nanofiber scaffolds and transferred onto the damaged corneal surface. Exp. Eye Res. 116, 312-323.

Den S., Sotozono C., Kinoshita S. and Ikeda T. (2004). Efficacy of early systemic betamethasone or cylosporine A after corneal alkali injury via inflammatory cytokine reduction. Acta Ophthalmol. Scand. 82, 195-199.

Dreier B., Thomasy S.M., Mendonsa R., Raghunathan V.K., Russell P. and Murphy C.J. (2013). Substratum compliance modulates corneal fibroblast to myofibroblast transformation. Invest. Ophthalmol. Vis. Sci. 54, 5901-5907.

Gordon G.M., Ledee D.R., Feuer W.J. and Fini M.E. (2009). Cytokines and signalling pathways regulating matrix metalloproteinase 9 (MMP9) expression in corneal epithelial cells. J. Cell Physiol. 221, 402-411.

Haber M., Cao Z., Panjwani N., Bedenice D., Li W.W. and Provost P.J. (2003). Effects of growth factors (EGF, PDGF-BB and TGF-beta 1) on cultured equine epithelial cells and keratocytes: Implications for wound healing. Vet. Ophthalmol. 6, 211-217.

Hoffart L., Matonti F., Conrath J., Daniel L., Ridings D., Masson G.S. and Chavane F. (2010). Inhibition of corneal neovascularization after alkali burn: comparison of different doses of bevacizumab in monotherapy or associated with dexamethasone. Clin. Exp. Ophthalmol., 38, 346-352.

Holan V., Chudickova M., Trosan P., Svobodova E., Krulova M., Kubinova S., Sykova E., Sirc J., Michalek J., Juklickova M., Munzarova M. and Zajicova A. (2011). Cyclosporine A-loaded and stem cell-seeded electrospun nanofibers for cell-based therapy and local immunosuppression. J. Control Release 156, 406-412.

Ishizaki M., Zhu G., Haseba T., Shafer S.S. and Kao W.W. (1993). Expression of collagen 1, smooth muscle alpha actin, and vimentin during the healing of alkali-burned and lacerated corneas. Invest. Ophthalmol. Vis. Sci. 34, 3320-3328.

Jester J.V., Petroll W.M. and Cavanagh H.D. (1999). Corneal stromal wound healing in refractive surgery: the role of myofibroblasts. Prog. Retin. Eye Res. 18, 311-356.

Jester J.V., Brown D., Pappa A. and Vasiliou V. (2012). Myofibroblast differentiation modulates keratocyte crystallin protein expression, concentration, and cellular light scattering. Invest. Ophthalmol. Vis. Sci. 53, 770-778.

Jiang T.S., Cai L., Ji W.Y., Hui Y.N., Wang Y.S., Hu D. and Zhu J. (2010). Reconstruction of the corneal epithelium with induced marrow mesenchymal stem cells in rats. Mol. Vis. 16,1304-1316.

Li F. and Zhao S.Z. (2014). Mesenchymal stem cells: Potential role in wound repair and transplantation. World J. Stem Cells 6, 296-304.

Luckett-Chastain L.R. and Galluci R.M. (2009). Interleukin (IL)-6 modulates transforming growth factor-β expression in skin and dermal fibroblasts from IL-6-deficient mice. Br. J. Dermatol. 161, 237-248.

Ma Y., Xu Y., Xiao Z., Yang W., Zhang C., Song E., Du Y. and Li L. (2006). Reconstruction of chemically burned rat corneal surface by bone marrow-derived human mesenchymal stem cells. Stem Cells 24, 315-321.

Pottecher J., Guillot M., Belaidi E., Charles A.L., Lejay A., Gharib A.Q., Diemunsch P. and Geny B. (2013). Cyklosporine A normalizes mitochondrial coupling, reactive oxygen species production and inflammation and partially restores skeletal muscle maximal oxidative capacity in experimental cross-clamping. J. Vasc. Surg, 57, 1100-1108.

Sekundo W., Augustin A.J. and Strempel I. (2002). Topical allopurinol or corticosteroids and acetylcysteine in the early treatment of experimental corneal alkali burns: a pilot study. Eur. J. Ophthalmol. 12, 366-372.

Seoane J. (2006). Escaping from the TGFbeta anti-proliferative control. Carcinogenesis 27, 2148-2156.

Sotozono C., He J., Matsumoto Y., Kita M., Imanishi J. and Kinoshita S. (1997). Cytokine expression in the alkali-burned cornea. Curr. Eye Res. 16, 670-676.

Sotozono C., He J., Tei M., Honma Y. and Kinoshita S. (1999). Effect of metalloproteinase inhibitor on corneal cytokine expression after alkali injury. Invest. Ophthalmol. Vis. Sci. 40, 2430-2434.

Sumioka T., Ikeda K., Okada Y., Yamanaka O., Kitano A. and Saika S. (2008). Inhibitory effect of blockinjg TGF-beta/Smad signal on injury-induced fibrosis of corneal endothelium. Mol. Vis. 14, 2272-2281.

Trosan P., Svobodova E., Chudickova M., Krulova M., Zajicova A. and Holan V. (2012). The key role of insulin-like growth factor I in limbal stem cell differentiation and the corneal wound-healing process. Stem Cells Dev., 21, 3341-3350.

Yao L., Li Z.R., Su W.R., Li Y.P., Lin M.L., Zhang W.X., Liu Y., Wan Q. and Liang D. (2012). Role of mesenchymal stem cells on cornea wound healing induced by acute alkali burn. PLoS One 7, e30842.

Yang Y., Wang Z., Yang H., Wang L., Gillespie S.R., Wolosin J.M., Bernstein A.M., Reinach P.S. (2013). TRRPV1 potentiates TGF beta-induction of corneal myofibroblast development through an oxidative stress-mediated p38-SSMAD2 signaling loop, Plos One 8, e77300.

Ye J., Yao K. and Kim J.C. (2006). Mesenchymal stem cell transplantation in a rabbit corneal alkali burn model: engraftment and involvement in wound healing. Eye 20, 482-490.

Ye J., Lee S.Y., Kook K.H. and Yao K. (2008). Bone marrow-derived progenitor cells promote corneal wound healing following alkali injury. Graefes Arch. Clin. Exp. Ophthalmol. 246, 217-222.

Yi K., Chung T.Y., Hyon J.Y., Koh J.W., Wee W.R. and Shin Y.J. (2011). Combined treatment with antioxidants and immunosuppressants on cytokine release by human peripheral blood mononuclear cells –chemically injured keratocyte reaction. Mol. Vis. 17, 2665-2671.

Wilson S.E. (2012). Corneal myofibroblast biology and pathobiology: Generation, persistence, and transparency. Exp. Eye Res. 99, 78-88.

Wu J., Chitapanarux T., Chen Y., Soon R.K. Jr. and Yee H.F. Jr (2013). Intestinal myofibroblasts produce nitric oxide in response to combinatorial cytokine stimulation. J. Cell. Physiol. 228, 572-580.

Zajicova A., Pokorna K., Lencova A., Krulova M., Svobodova E., Kubinova S., Sykova E., Pradny M., Michalek J., Svobodova J., Munzarova M. and Holan V. (2010). Treatment of ocular surface

injuries by limbal and mesenchymal stem cells growing on nanofiber scaffolds. Cell Transpl. 19, 1281-1290.

Zhang X.L., Topley N., Ito T. and Phillips A. (2005). Interleukin-6 regulation of transforming growth factor (TGF)-beta receptor compartmentalization and turnover enhances TGF-beta1 signaling. J. Biol. Chem. 280, 1239-1245.

Accepted January 22, 2016